MECHANICAL CALCULATION MODEL FOR WELDED HOLLOW SPHERICAL JOINT IN SPATIAL LATTICED STRUCTURES

Yang Ding [1], Lin Qi [2,*], Zhongxian Li [3]

[1] *Professor, Department of Civil Engineering, Tianjin University, Tianjin, China*
[2] *Ph. d candidate, Department of Civil Engineering, Tianjin University, Tianjin, China*
[3] *Professor, Department of Civil Engineering, Tianjin University, Tianjin, China*
**(Corresponding author: E-mail: qilin1208@163.com)*

Received: 25 January 2011; Revised: 16 March 2011; Accepted: 24 March 2011

ABSTRACT: The welded hollow spherical joint has been extensively applied in spatial latticed structures in China. Currently the welded hollow spherical joint is generally modeled by rigid connection. No matter what great loads the structure bears, deformations at the ends of members connected by the same welded hollow spherical joint remain the same. However, in some cases the welded hollow spherical joint could rupture which results in the damage of the structure. Therefore, mechanical calculation model for welded hollow spherical joint should be established for the refined simulation of spatial latticed structures. In this paper multi-step finite element analysis model for welded hollow spherical joint is established. Mechanical behaviors of the joint under cyclic loads can be simulated by this model, and numerical calculation results correspond well with the experiment data. Numerical analysis indicates that when compression load is applied to the welded hollow spherical joint, the strain energy can be transferred in the sphere, and the joint will not rupture. When tension load is applied, deformations of the welded hollow spherical joint concentrate in the area where the tube meets the sphere. The strain energy accumulates continuously there and the joint ruptures when the local stress reaches ultimate shear strength. Mechanical calculation model for welded hollow spherical joint, by which the repeated loading-unloading processes and failure process of the joint under seismic excitations can be simulated, is established by parameter analysis. Numerical calculation results indicate that welded hollow spherical joints of single layer lamella grid cylindrical latticed shell could rupture under strong earthquakes, and the structure damages subsequently due to the topological structure transformation. Bearing capacities of welded hollow spherical joints under strong earthquake can be overestimated if they are modeled by rigid connection. The compression load applied to the joint cannot be bigger than the critical buckling loads of the connected member, so the compression load that the joint carries will not reach its ultimate compression load generally.

Keywords: Welded hollow spherical joint, Mechanical calculation model, Finite element analysis model, Rupture, Failure mechanism, Structural damage

1. INTRODUCTION

The welded hollow spherical joint was invented and first used in Tianjin Science & Technology Hall in 1965 (Makowski [1]). Nowadays, this pattern of joint is extensively applied in spatial latticed structures in China. The ultimate bearing capacity and failure mechanism of welded hollow spherical joint is a major research area. Liu [2] introduced the research and application of welded hollow spherical joints of spatial latticed structures in China. Han and Liu [3] calculated the tension and compression ultimate loads of welded hollow spherical joints by three-dimensional degenerated curved shell elements. They also proposed a calculation method for the joint under bending moments or eccentric loads and analyzed the influence of the stiffening rib on the ultimate bearing capacity of the joints (Han et al. [4]). Li [5] investigated the structural behavior and load-carrying capacity of welded hollow spherical joints connected with rectangular or square steel tubes under axial forces, bending moments and combined loading of the two. Qiu, Xue and Feng [6] investigated the fire performances of welded hollow spherical joints with the thermal parameters specified in the EUROCODE 3 [7] and ISO 834 [8] experimentally and numerically. Based on the experimental investigation, Chen [9] propounded that the welded hollow spherical joint under tension load damaged due to the material failure, and that under compression load damaged due to the instability of the sphere. Xue [10] propounded that it was the plastic zone where the tube met the sphere that caused the failure of the joint under compression load. Current research on welded hollow spherical joint focuses on the ultimate bearing capacity calculation equations for the joint under monotone load, which are applicable in static designs. However, when subject to seismic excitations, the welded hollow spherical joint undergoes a loading-unloading process repeatedly, and the mechanical behaviors of it are in a state of flux. So the equations derived from the monotone loading are no longer applicable. Currently the welded hollow spherical joint is generally modeled by rigid connection. No matter what great loads the structure bears, deformations at the ends of members connected by the same joint keep the same. However, in some cases the welded hollow spherical joint could rupture which results in the damage of the structure. The bearing capacity of structure under strong seismic excitations will be overestimated if welded hollow spherical joints are simply modeled by rigid connections. In this paper multi-step finite element analysis model for welded hollow spherical joint is established, and its failure mechanism is analyzed. By parameter analyses the mechanical calculation model for welded hollow spherical joint is established. The repeated loading-unloading process and failure process of the joint under seismic excitation can be simulated by this model.

2. FINITE ELEMENT ANALYSIS MODEL

Members of the spatial latticed structure bear the axial forces mainly, so it is the axial force that transfers to the welded hollow spherical joint mostly. Based on the experimental and theoretical investigations, CHI, Deierlein and Ingraffea [11] indicated that the ultimate bearing capacity of welded hollow spherical joint under single direction axial force was almost the same as the ultimate bearing capacity of that under multi-direction axial force. Based on the experimental data, Chen [9] and Xue [10] found that the compression load-displacement curve of welded hollow spherical joint declined rapidly after reaching the peak value. In this stage, the joint deforms quickly and the stable experimental data are difficult to acquire. Therefore, finite element analysis model composed of axisymmetric elements of ABAQUS considering the nonlinearities of both material and geometry is used to analyze the mechanical calculation model of welded hollow spherical joint in this paper. Load increment method, displacement increment method and arc-length method are all used to establish the multi-step finite element analysis model of the joint under single direction cyclic axial load. The finite element analysis model is illustrated in Figure 1.

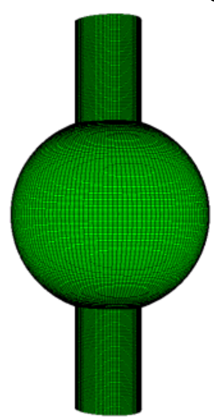

Figure 1. Finite Element Analysis Model of Welded Hollow Spherical Joint

There is a load-vertical displacement curve of the weld toe of welded hollow spherical joint with decline segment derived from experiment in literature [10]. The joint is composed of steel tube of Φ150×22 and sphere of D400×14. Both of the experimental curve and numerical simulation curve calculated by finite element analysis model using the experimental material parameters are plotted in Figure 2. The two curves match well and have a maximum relative error of just 2.65%. So the finite element analysis model is of good accuracy and can be used for the further analysis.

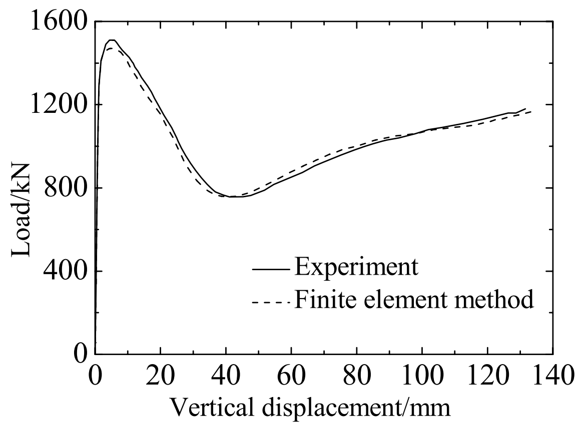

Figure 2. Comparison of the Load-vertical Displacement Curves of the Weld Toe of the Joint

3. CHARACTERISTICS OF LOAD-DISPLACEMENT CURVE OF THE JOINT

Envelop of the load-displacement curve of the welded hollow spherical joint needs to be established to analyze the mechanical behaviors of the joint under seismic excitations. The characteristics of load-displacement curve can be analyzed and the mechanical calculation model can be established accordingly.

Take the welded hollow spherical joint composed of steel tube of Φ168×10 and sphere of D500×16 as an instance. Apply compression force to the joint firstly and make it cave in. Segment O-A-B-C-D-E of the load-displacement curve in Figure 3 corresponds to this process. The load corresponding to point A, which is an extremum of the curve, is the ultimate compression load of the joint. The plastic zone forms where the tube meets the sphere and extends outward then. In segment A-B the upper spherical crown caves in rapidly with the decrement of compression load. Experimental photo and finite element model of the state at point B are respectively illustrated in Figure 4a and Figure 4b. They exhibit a same deformation pattern. Material of the annular area marked by the letter N in Figure 4b yields at the state of point B. In segment B-C the joint deforms steadily, and both the compression load and the deformation increase. The joint reaches the ultimate bearing state again at point C with a load equal to that of point A. The nether spherical crown caves in as well in segment B-C. The sectional view of the joint at the state of point C is illustrated in Figure 4c, and material of the annular areas marked by the letters N and P yields. In segment C-D the joint deforms unsteadily again, and the deformation increases rapidly with the decrement of compression load. The deformation of the joint turns steady at point D with a load equal to that of point B. In segment D-E the joint deforms greatly with an appearance of drum which is illustrated in Figure 4d. Both the compression deformation and compression load increase in segment D-E until the inner surfaces of the joint contact at point E. E-F is the unloading segment with a same slope as segment O-A. Residual compression deformation with an amount equal to the length of segment O-F remains at point F (Figure 4e). Displacement increment method is employed in the tension process which corresponds to segment G-H-I-J-K-L. Segment G-H-I-J-K is the opposite process of segment A-B-C-D-E. In segment J-K the joint is tensioned to the original figuration. A slight tension deformation forms at point K which is illustrated in Figure 4f. The plastic zone then forms where the tube meets the sphere under the tension load, which results in the nonlinearity of segment K-L. The joint ruptures at point L under the ultimate tension load. Experimental photo and finite element model of the failure joint, which are respectively illustrated in Figure 4g and Figure 4h, exhibit great congruity.

If unloading occurs at points B, C or D before the inner surfaces of the joint contact, the unloading paths will be B-B′, C-C′ or D-D′ respectively with the same slope as segments O-A and E-F. Compression residual deformations with amounts equal to the lengths of segments O-B′, O-C′ or O-D′ respectively remain at the unloading completing points B′, C′ or D′. If then compression load is applied to again, the joint deforms following the paths B′-B-C-D-E, C′-C-D-E or D′-D-E. If then tension load is applied to, the joint deforms following the paths B′-J-K-L, C′-I-J-K-L or D′-H-I-J-K-L.

If tension load is applied to firstly, the joint will deform following the path O-K-L. O-K is the elastic loading segment with the same slopes as segments O-A and E-F. It is the elastic process if unloading occurs in segment O-K. If the unloading occurs in segment K-L, at point L′ for example, the unloading path will be L′-M with the same slope as segments O-A, O-K and E-F. Tension residual deformation with an amount equal to the length of segment O-M remains at point M.

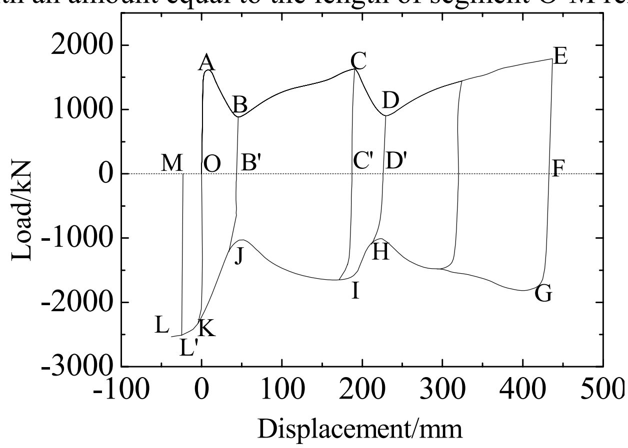

Figure 3. Envelope of Load-displacement Curve of the Joint

4. FAILURE MECHANISM OF WELDED HOLLOW SPHERICAL JOINT

No matter the welded hollow spherical joint is tensioned or compressed, it is the junction where the tube meets the sphere yields at firstly. Under compression load, the sphere can cave in and deform largely. Most area of the sphere deforms, and the plastic zone extends outward from the junction. The strain energy transfers in the sphere, so the welded hollow spherical joint will not rupture under compression load. Under tension load, the tension deformation of the joint is restricted. The plastic zone at the tube-sphere junction cannot extend outward. So strain energy accumulates at the junction until the joint ruptures. Therefore, a conclusion can be drawn that the welded hollow spherical joint can rupture under tension load, while it will not rupture under compression load even with a large deformation. This is consistent with the experiment results [9, 10].

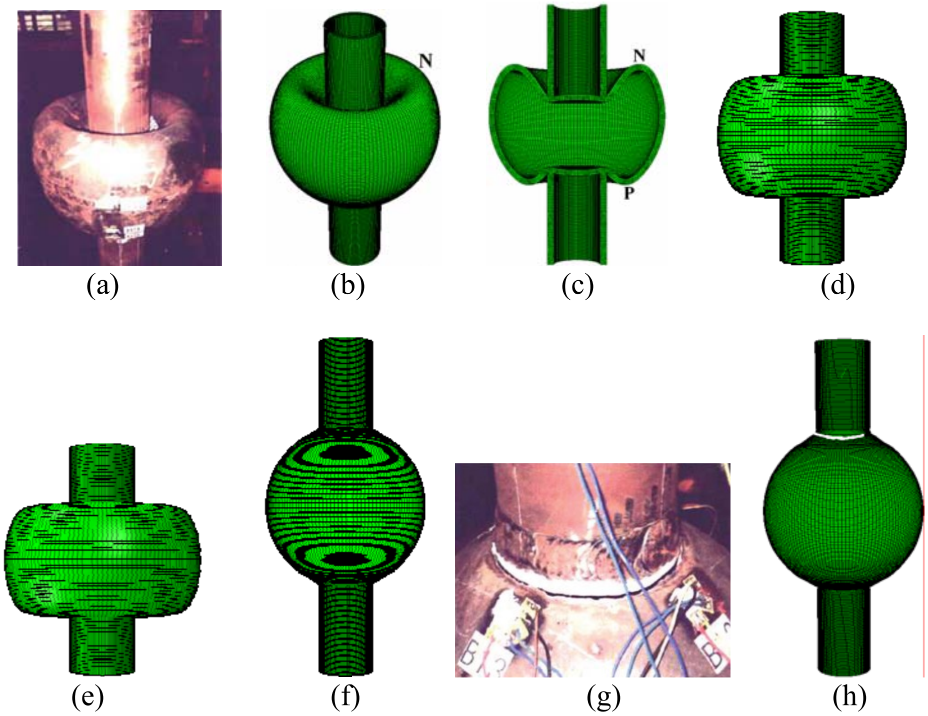

Figure 4. Deformations of the Joint

5. MECHANICAL CALCULATION MODEL FOR WELDED HOLLOW SPHERICAL JOINT

According to the analyses in Section 3, mechanical calculation model for welded hollow spherical joint can be summarized as Figure 5, which is a mathematical description of the envelop of load-displacement curve in Figure 3. In Figure 5, all the slopes of segments O-A, O-K, B-J, C-I, D-H, E-G and M-L are k. Slopes of segments H-I, J-K are both k_1. Slopes of segments A-B, C-D are both $-k_1$. Slopes of segments B-C, D-E are both k_2. Slopes of segments G-H, I-J are both $–k_2$. Slope of segments K-L is k_3. The load P_1, which corresponds to points A and C, is the ultimate compression load of the joint. The load corresponding to points B and D is P_2. The load corresponding to points H and J is $-P_2$. The load corresponding to points I and K is $-P_1$. The load P_3, which corresponds to point L, is the ultimate tension load of the joint. The abscissa l corresponding to point E is the compression displacement when the inner surfaces of the joint contact. When residual deformation occurs, the enclosed part of the envelope translates along the horizontal axis by an amount equal to the residual deformation.

The mechanical calculation model of welded hollow spherical joint can be defined by P_1, P_2, P_3, k, k_1, k_2, k_3 and l.

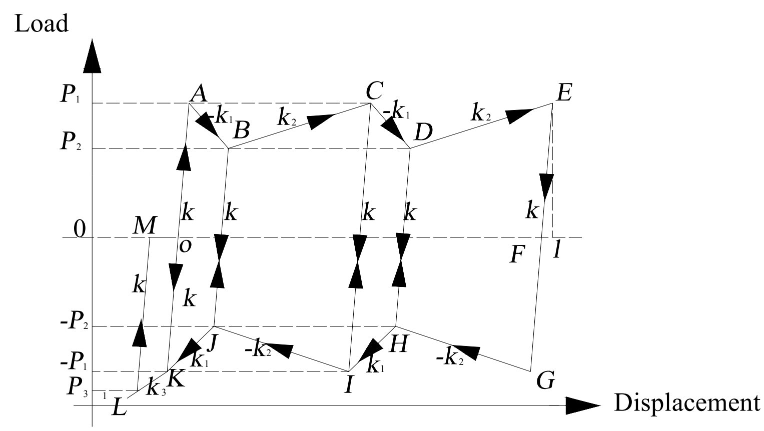

Figure 5. Mechanical Calculation Model of Welded Hollow Spherical Joint

Diameter D and thickness t of the sphere, yielding strength f_y and ultimate strength f_u of the steel, and diameter d of the tube are relevant to the mechanical behavior of the welded hollow spherical joint other than the thickness of the tube [12]. Finite element analysis models of 42 welded hollow spherical joints of parameters listed in Table 1 are established to determine the mechanical calculation model. $20 \le D/t \le 35$, it is strictly constrained in the bound stated in literature [12] to keep the stability of the sphere. $2.4 \le D/d \le 3.6$, it is appropriately relaxed for a broader parameter analysis.

Table 1. Parameters of Welded Hollow Spherical Joints

No.	1	2	3	4	5	6	7	8	9	10	11	12	13	14
D/mm	480	520	560	600	640	680	720	600	600	600	600	600	600	600
t/mm	22	22	22	22	22	22	22	18	20	22	24	26	28	30
d/mm	200	200	200	200	200	200	200	200	200	200	200	200	200	200
Steel	Q345	Q345	Q345	Q345	Q345	Q345	Q345	Q345	Q345	Q345	Q345	Q345	Q345	Q345
No.	15	16	17	18	19	20	21	22	23	24	25	26	27	28
D/mm	600	600	600	600	600	600	600	480	520	560	600	640	680	720
t/mm	22	22	22	22	22	22	22	22	22	22	22	22	22	22
d/mm	176	188	200	212	224	236	248	200	200	200	200	200	200	200
Steel	Q345	Q345	Q345	Q345	Q345	Q345	Q345	Q235	Q235	Q235	Q235	Q235	Q235	Q235
No.	29	30	31	32	33	34	35	36	37	38	39	40	41	42
D/mm	600	600	600	600	600	600	600	600	600	600	600	600	600	600
t/mm	18	20	22	24	26	28	30	22	22	22	22	22	22	22
d/mm	200	200	200	200	200	200	200	176	188	200	212	224	236	248
Steel	Q235	Q235	Q235	Q235	Q235	Q235	Q235	Q235	Q235	Q235	Q235	Q235	Q235	Q235

Envelops of load-displacement curves of joints 1-7, in which only D changes among all the parameters, are plotted in Figure 6a. Qualitative analysis indicates that P_1, P_2, k, k_1, k_2 and k_3 get smaller with the increment of D. Envelops of load-displacement curves of joints 8-14, in which only t changes among all the parameters, are plotted in Figure 6b. Qualitative analysis indicates that P_1, P_2, k, k_1, k_2 and k_3 get bigger with the increment of t. Envelops of load-displacement curves of joints 15-21, in which only d changes among all the parameters, are plotted in Figure 6c. Qualitative analysis indicates that with the increment of d, P_1, P_2, k, k_1 and k_3 get bigger and k_2 gets smaller. Envelops of load-displacement curves of joints 1 and 22, in which only the steel type changes among all the parameters, are plotted in Figure 6d. Qualitative analysis indicates that P_1, P_2, k, k_1, k_2 and k_3 get bigger with the increment of yielding strength of the steel.

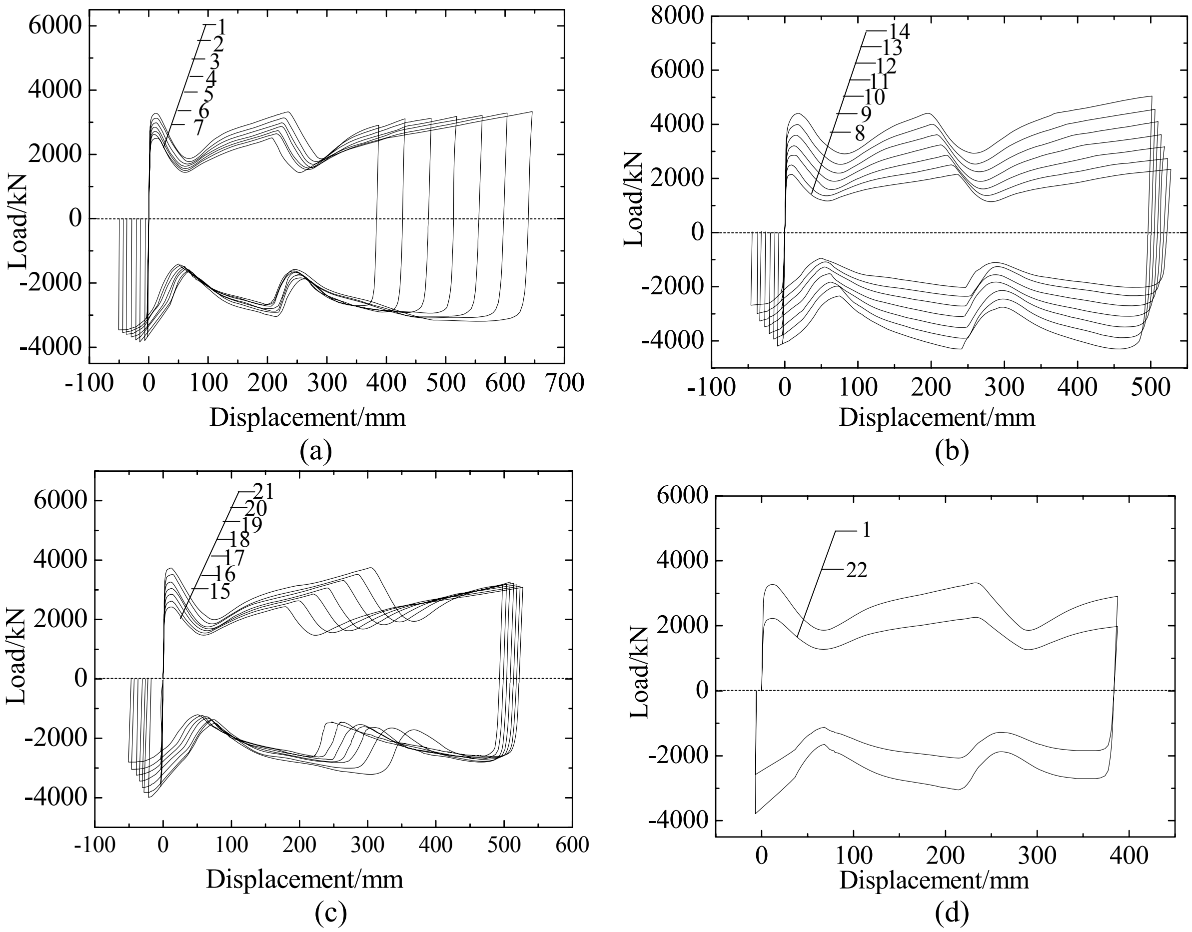

Figure 6. Envelopes of Load-displacement Curves of Parametric Joint Models

Quantitatively analyze the 42 envelops of load-displacement curves of the parametric joint models. The curve with abscissa of dimensionless variable td/D^2 and ordinate of dimensionless variable $P_1/\pi tdf_y$ is plotted in Figure 7a. The two variables are linearly related with the linear correlation coefficient of 0.98. By least square method, the linear regression equation of P_1 can be derived

$$P_1 = (0.40 + 15.88\frac{td}{D^2})\pi tdf_y \tag{1}$$

The curve with abscissa of variable td/D and ordinate of variable $P_2/\pi tf_y$ is plotted in Figure 7b. The two variables with the same dimension of L are linearly related with the linear correlation coefficient of 0.99. By least square method, the linear regression equation of P2 can be derived

$$P_2 = (0.02 + 7.14\frac{td}{D})\pi tf_y \tag{2}$$

The curve with abscissa of variable td/D and ordinate of variable k/f_y is plotted in Figure 7c. The two variables with the same dimension of L are linearly related with the linear correlation coefficient of 0.98. By least square method, the linear regression equation of k can be derived

$$k = (-0.61 + 397.71\frac{td}{D})f_y \tag{3}$$

The curve with abscissa of variable td/D and ordinate of variable k_1/f_y is plotted in Figure 7d. The two variables with the same dimension of L are linearly related with the linear correlation coefficient of 0.97. By least square method, the linear regression equation of k1 can be derived

$$k_1 = (0.04 + 6.93\frac{td}{D})f_y \tag{4}$$

The curve with abscissa of dimensionless variable t^2/Dd and ordinate of dimensionless variable k_2/tf_y is plotted in Figure 7e. The two variables are linearly related with the linear correlation coefficient of 0.97. By least square method, the linear regression equation of k2 can be derived

$$k_2 = (0.92 + 103.59\frac{t^2}{Dd})tf_y \tag{5}$$

The curve with abscissa of variable td/D and ordinate of variable k_3/f_y is plotted in Figure 7f. The two variables with the same dimension of L are linearly related with the linear correlation coefficient of 0.99. By least square method, the linear regression equation of k3 can be derived

$$k_3 = (0.08 + 15.52\frac{td}{D})f_y \tag{6}$$

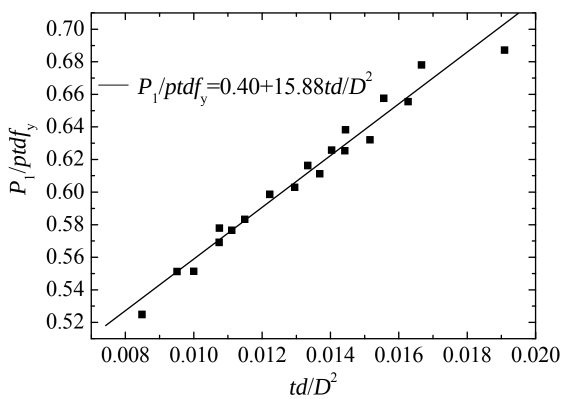

(a)

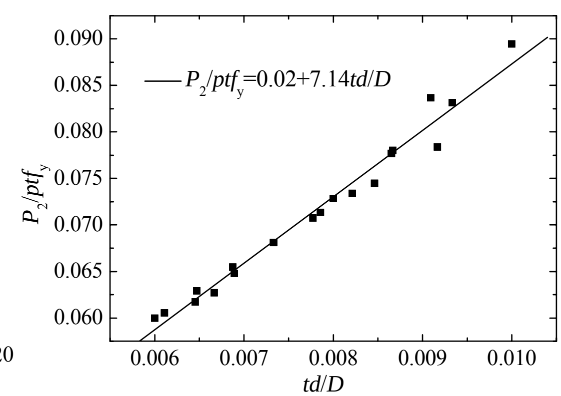

(b)

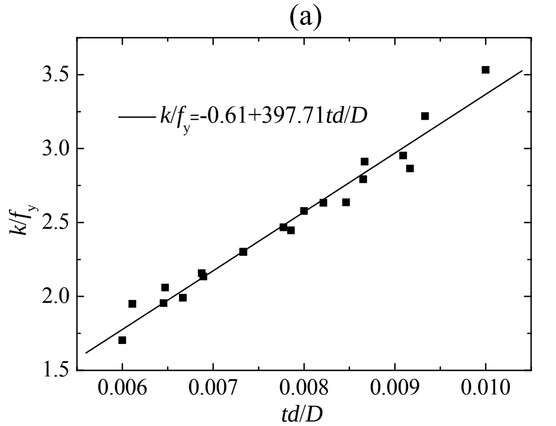

(c)

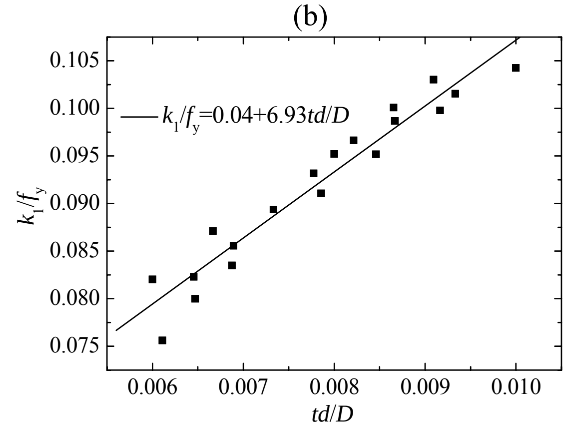

(d)

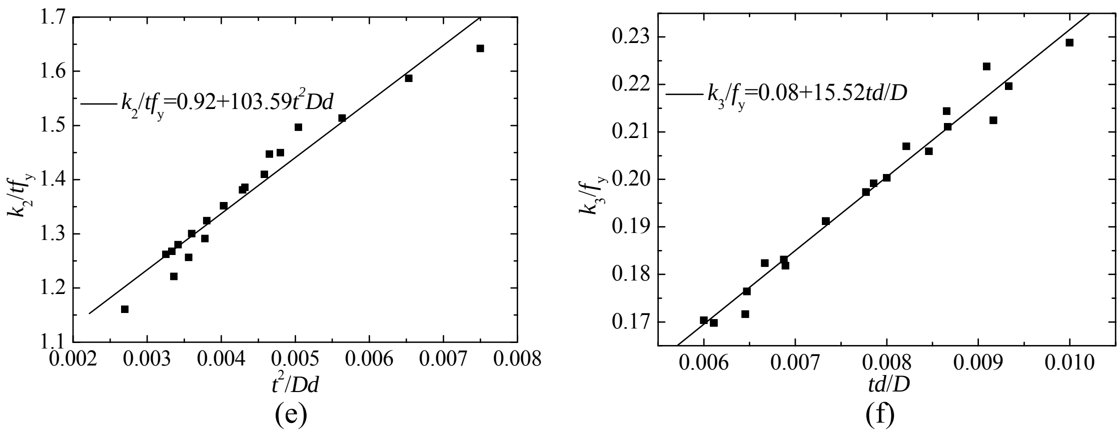

Figure 7. Parameter Analyses of Mechanical Calculation Model for the Joints

When the welded hollow spherical joint is subjected to ultimate tension load P_3, punching shear failure occurs where the tube meets the sphere. Shear stress in the punching shear surface reaches the shear strength $f_u/\sqrt{3}$. The height of the punching shear surface is δ which is marked in Figure 8. Based on the force equilibrium equation the expression of P_3 can be derived

$$P_3 = \frac{\pi d \delta f_u}{\sqrt{3}} = \frac{\pi d f_u(\sqrt{D^2-d^2} - \sqrt{(D-2t)^2-d^2})}{2\sqrt{3}} \tag{7}$$

Based on the geometrical relationship, the expression of l, which is the distance between the contact points in the inner surface of welded hollow spherical joint, can be derived

$$l = \sqrt{(D-2t)^2 - d^2} \tag{8}$$

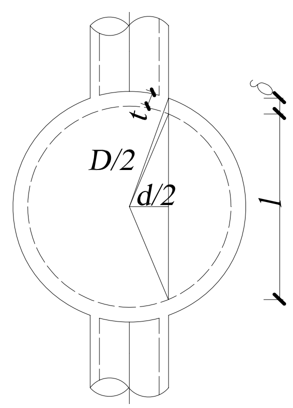

Figure 8. Geometrical Parameters of the Joint

Mechanical calculation model of the welded hollow spherical joint can be defined by Eq. 1-8. Ultimate tension loads of welded hollow spherical joints of the experiment [9, 10] and those calculated by mechanical calculation model in this paper using experimental material parameters are presented in Table 2. Ultimate compression loads of welded hollow spherical joints of the experiment [9, 10] and those calculated by mechanical calculation model in this paper using the experimental material parameters are presented in Table 3. The results of experiment and numerical calculation correspond well and have a maximum relative error less than 5%. Therefore, the mechanical calculation model of welded hollow spherical joint in this paper is of good accuracy.

Table 2. Comparisons of the Ultimate Tension Loads of the Joints

No.	*D*/mm	*t*/mm	*d*/mm	Steel	Ultimate tension loads /kN		Relative error/%
					Experiment	Mechanical calculation model	
1	200	6	89	Q235	432.00	436.10	0.95
2	300	10	108	Q235	864.00	844.41	-2.27
3	400	12	130	Q235	1250.00	1201.36	-3.89
4	400	18	130	Q235	1852.00	1805.83	-2.49
5	450	16	159	Q235	2020.00	1983.94	-1.79
6	500	14	160	Q235	1684.00	1721.26	2.21
7	300	8	102	Q345	845.59.00	837.24	-0.99
8	400	14	150	Q345	2271.65	2191.32	-3.54

Table 3. Comparisons of the Ultimate Compression Loads of the Joints

No.	*D*/mm	*t*/mm	*d*/mm	Steel	Ultimate compression loads /kN		Relative error/%
					Experiment	Mechanical calculation model	
1	200	6	89	Q235	314.00	302.78	-3.57
2	250	8	108	Q235	480.00	495.91	3.32
3	280	6	159	Q235	522.00	524.33	0.45
4	300	10	108	Q235	583.00	590.91	1.36
5	500	20	219	Q345	3700.00	3731.79	0.86
6	650	25	219	Q345	4000.00	4166.50	4.16
7	300	8	102	Q345	570.99	571.56	0.10
8	400	14	150	Q345	1708.46	1645.21	-3.70

Vertical dynamic load plotted in Figure 9 is applied to the welded hollow spherical joint composed of steel tube of Φ150×6 and sphere of D400×14. Vertical displacement time history curves of the joint weld toe based on the solid finite element model and the mechanical calculation model in this paper are plotted in Figure 10. The two curves correspond well, and the calculation time taken by the mechanical calculation model method is just 1/600 of that taken by solid finite element model method. Therefore, the mechanical calculation model of welded hollow spherical joint is of good efficiency and can be used in the calculation of structural dynamic responses.

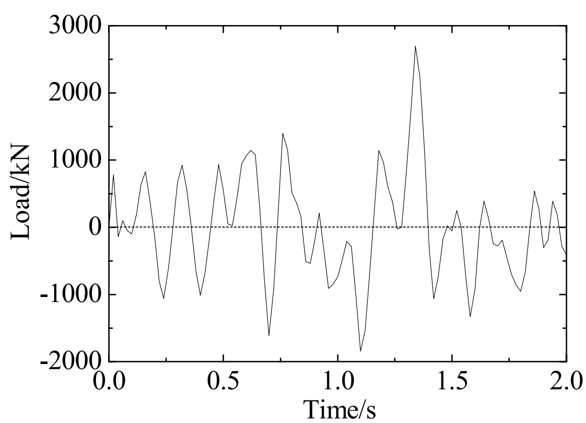

Figure 9. Time History of Vertical Dynamic Load

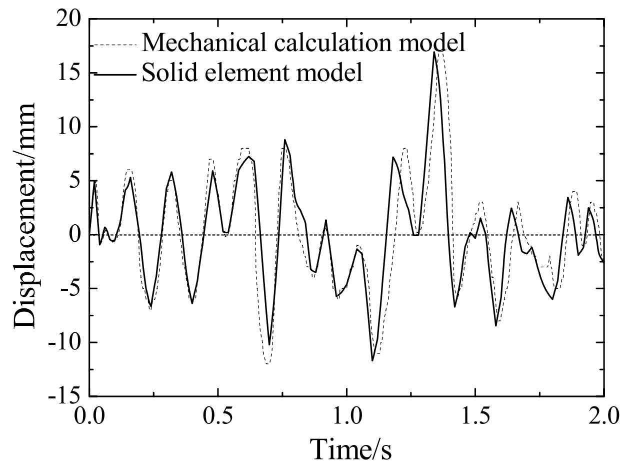

Figure 10. Time History of Vertical Displacement

6. APPLICATION

A lamella grid single layer cylindrical latticed shell with the span of 15m, the length of 30m and the rise-span ratio of 1/5 is taken as an example. The structure is supported along four sides, and the plan view is illustrated in Figure 11. The structure consists of circular tubes of Φ89×3, Φ102×3.5 and Φ114×3.5, and welded hollow spherical joints of WS2406 (diameter of 240mm and thickness of 6mm) and WS2808 (diameter of 280mm and thickness of 8mm). Material of the structure is Q235 (yielding strength is 235 MPa). The structure bears surface load of 2.00kN/m^2 and three-direction seismic excitations of El-Centro wave with peak acceleration of 900gal and duration of 15s.

Numerical calculation results indicate that the junction where member 18 meets the sphere of the joint (marked by black dot in Figure 11) ruptures at 11.46s. Then the tube-sphere junctions of members 21, 206, 208, 210 and 212 (marked by black dots in Figure 11) rupture at 11.82s, 11.83s, 11.86s, 11.94s and 11.98s respectively. At 12.90s the structure damages due to the topological transformation. Plan view of the damaged structure (Figure 12) shows that some members disconnect from the welded hollow spherical joints, and the structural grids twist severely. Axial force time history curves of member 21 and 206 are respectively plotted in Figure 13 and Figure 14. The two members disconnect from the joints when axial forces reach 350.06kN and 406.26kN respectively, which are the very ultimate tension loads of the welded hollow spherical joints they are connected to. Compression axial forces in the two members decrease rapidly when reaching 125.02kN and 153.46kN respectively. It corresponds to the buckling processes of the two members with critical buckling axial forces of 125.02kN and 153.46kN respectively. Therefore, the maximum compression load applied to the joint will not exceed the critical buckling loads of the connected members. Based on Eq. (1) ultimate compression loads of the welded hollow spherical joints that member 21 and 206 connected to are 256.88kN and 297.12kN respectively, which are far greater than the critical buckling loads of the two members. Therefore, the compression load the welded hollow spherical joint bears will not exceed its ultimate compression load generally in spatial latticed structures. The ultimate tension load of the member is determined by material strength. The ultimate tension load of member 21 and 206 are 367.48kN and 425.03kN respectively, which are greater than the ultimate tension loads of welded hollow spherical joints the two members connect to. Therefore, the welded hollow spherical joints of the spatial latticed structures may failure under strong earthquakes.

If welded hollow spherical joints are simply modeled by rigid connections, the plan view of the deformed structure at 13s when the earthquake stops (Figure 15) shows that the conjoint ends of the members are connected all along and none of the joints failures. Bearing capacity of the structure subjected to strong seismic excitations is overestimated in this case.

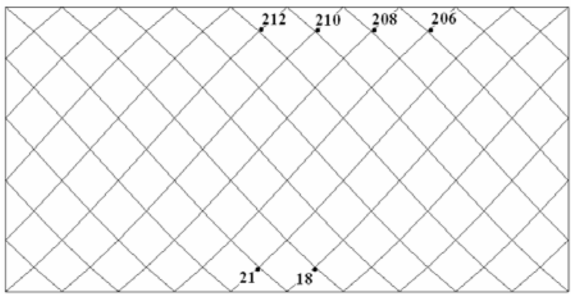

Figure 11. Plane View of the Structure

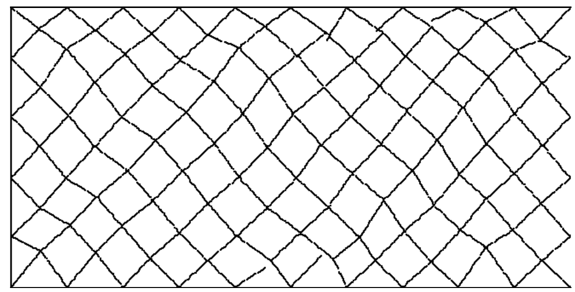

Figure 12. Plane View of the Damaged Structure

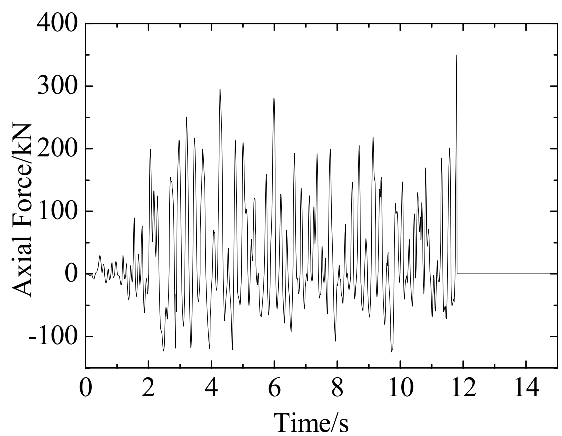

Figure 13. Time History of Axial Force of Member 21

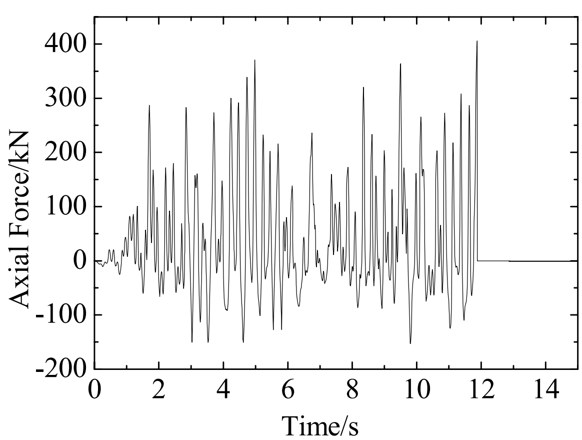

Figure 14. Time History of Axial Force of Member 206

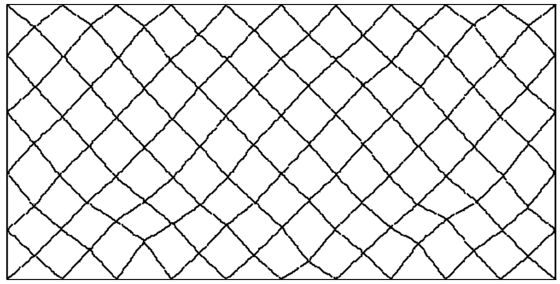

Figure 15. Deformation of the Structure when Joints are Modeled by Rigid Connections

7. CONCLUSIONS

The mechanical calculation model for welded hollow spherical joint in spatial latticed structures is studied in this paper. Based on the analyses, some conclusions can be drawn as follows:

Finite element analysis model composed of axisymmetric elements of ABAQUS considering the nonlinearities of both material and geometry is used to analyze the mechanical calculation model of welded hollow spherical joint. Load increment method, displacement increment method and arc-length method are all used to establish the multi-step finite element analysis model of welded hollow spherical joint subjected to single direction cyclic axial load. Numerical calculation results by the multi-step finite element analysis model match well with the empirical results.

Numerical analyses indicate that when compression load is applied to the welded hollow spherical joint, the strain energy can be transferred in the sphere, and the joint will not rupture. When tension load is applied to the joint, the deformation is restricted, and the strain energy accumulates continuously at the tube-sphere junction. The joint ruptures when the local stress reaches ultimate shear strength.

Envelop of the load-displacement curve of welded hollow spherical joint is established and the characteristics of the load-displacement curve is analyzed. Mechanical calculation model for welded hollow spherical joint is established by parameter analysis. By this model the repeated loading-unloading process and failure process of the joint under seismic excitations can be simulated.

Numerical calculation results indicate that some welded hollow spherical joints of single layer lamella grid cylindrical latticed shell will rupture under strong earthquakes, and the structure damages due to the topological transformation. Bearing capacity of welded hollow spherical joints under strong earthquakes can be overestimated if they are modeled by rigid connections. The compression load applied to the joint cannot be bigger than the critical buckling loads of the connected members, so the compression load that the joint carries will not reach its ultimate compression load generally.

ACKNOWLEDGEMENTS

Financial supports from National Natural Science Foundation of China (Grant No. 90715034 and 50978181), Program for New Century Excellent Talents in University, Ministry of Education of China (Grant No. NCET-06-0229), and Program for Applied Foundation and Advanced Technology, Tianjin, China (Grant No. 09JCZDJC25200) are gratefully acknowledged.

REFERENCES

[1] Makowski, Z.S., "Analysis, Design and Construction of Double-layer Grids", London, Applied Science Publishers Ltd, 1981.

[2] Liu, X.L., "Research and Application of Various Joints of Space Grid Structures in China", Proceedings of the IASS-ASCE International Symposium 1994 on Spatial, Lattice and Tension Structures, Atlanta, GA, USA, 1994, pp. 221-228.

[3] Han, Q.H., Liu X.L., "Ultimate Bearing Capacity of the Welded Hollow Spherical Joints in Spatial Reticulated Structures", Engineering Structures, 2004, Vol. 26, No. 1, pp. 73-82.

[4] Han, Q.H., Zhou, Q.Z. and Chen, Y., et al., "Ultimate Bearing Capacity of Hollow Spherical Joints Welded with Circular Pipes under Eccentric Loads", Transactions of Tianjin University, 2007, Vol. 13, No. 1, pp. 28-34.

[5] Li, X., "Load-carrying Capacity and Practical Design Method of Welded Hollow Spherical Joints in Space Latticed Structures", Advanced Steel Construction, 2010, Vol. 6, No. 4, pp. 976-1000.

[6] Qiu, L.B., Xue, S.D. and Feng, M., "Fire Performance of Space Grid Structures", Journal of the International Association for Shell and Spatial Structures, 2009, Vol. 50, No. 162, pp. 151-160.

[7] Eurocode 3: Design of steel structures—Part1-2: General rules-Structural fire design. EN 1993-1-2. London: BSI, 2005.

[8] International Standards Organization: Fire-resistance test — Elements of building construction (ISO 834-1), 1999.

[9] Chen, Z.H., "Analysis of Collapse Mechanism and Experiment Study on Load Capacity of Welded Hollow Sphere Joint in Space Grids", Dissertation for Master Degree of Tianjin University, Tianjin, China, 1990. (in Chinese)

[10] Xue, W.L., "Load-carrying Capacity and Practical Design Method of Welded Hollow Spherical Joints Connected with Circular Steel Tube", Dissertation for Doctor Degree of Tongji University, Shanghai, China, 2008. (in Chinese)

[11] Chi, W.M., Deierlein, G.G. and Ingraffea, A., "Fracture Toughness Demands in Welded Bean-column Moment Connections", Journal of Structural Engineering, 2000, Vol. 126, No. 1, pp. 88-97.

[12] Chinese Technical Specification for Space Frame Structures (JGJ 7-2010), China, 2010. (in Chinese)